Analytical Methods

Accepted Manuscript

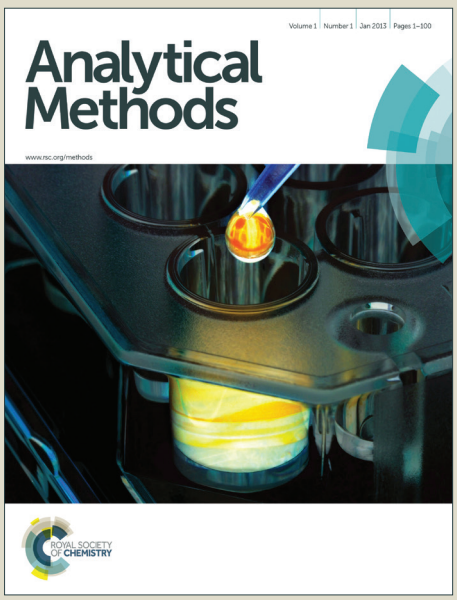

ROYAL SOCIETY OF CHEMISTRY

www.rsc.org/methods

Synthesis of Novel Quantum Dots from DNA under Mild Conditions and Used as a Fluorescent Probe for Detection of Fe^{3+} and Biological Imaging

Guifang Cheng[1], Weibo Zhang[1], Ying Zhou[1], Qifeng Ge[2], Chaobiao Huang*[1]

[1]*College of Chemistry and Life Science, Zhejiang Normal University,*

[2]*Zhejiang Normal University Xingzhi College, Jinhua 321004, China*

*Corresponding author: *Chaobiao Huang, E-mail: hcb@zjnu.cn*

Abstract

A simple method for the synthesis of water-soluble and well-dispersed fluorescent DNA-dots under mild conditions is reported. The solution of DNA-dots shows blue fluorescence and luminescence lifetime equals to 2.74ns, with a quantum yield up to 7.5%. It is attractive that DNA-dots can be used as an effective fluorescent probe for the detection of iron ions with relatively good selectivity and sensitivity in an aqueous solution as well as biological imaging applications.

Keywords: DNA-dots, Mild Conditions, Fluorescent Probe, Biological Imaging

Introduction

Fluorescent nanoparticles have attracted increasing interest on research due to their chemical inertness, optical stability, high luminous efficiency, easily modification[1-4] as well as their promising applications in electrooptics and bionanotechnology[5]. The fluorescence nanomaterials mainly include semiconductor quantum dots, noble metal nanoclusters as well as carbon nanomaterials. As far as we

know, the semiconductor quantum dots have toxic effect on cells due to the presence of Cd, Pb[6-8]. Noble metal nanoclusters have been receiving enormous attention. Nevertheless, their optical properties are influenced by many factors, particularly the heavy metal ions, sulfhydryl compounds as well as oxidation agent[9-11].

To the best of our knowledge, there have been few reports on the synthesis of quantum dots using a DNA source. In this research, we developed a simple route to synthesize DNA quantum dots (DNA-dots) at a relatively low reaction temperature. It is found that the DNA-dots are water-soluble and exhibit a relatively strong fluorescence. Moreover, the as-obtained DNA-dots can sensitively and selectively detect Fe^{3+} ions in the presence of Ag^{+}, Na^{+}, Cd^{2+}, Co^{2+}, Zn^{2+}, Ni^{2+}, Ca^{2+}, Fe^{2+}, Mn^{2+}, Cu^{2+}, Hg^{2+} Mg^{2+}, $Cr^{3+}$and Al^{3+}, which offers a novel sensing plat form for the detection of Fe^{3+} ions.

Experimental section

Reagents

Deoxyribonucleic acid sodium salt (from salmon testes) was purchased from Sigma-Aldrich. NaCl、$NiCl_2·6H_2O$、$CuCl_2·2H_2O$、$MgCl_2·6H_2O$、$HgCl_2$、$CdCl_2$、$AgNO_3$、$FeCl_3$、$ZnCl_2$、$CoCl_2·6H_2O$、$CrCl_3·6H_2O$、$CaCl_2·2H_2O$、$AlCl_3·6H_2O$、$FeCl_2·4H_2O$、$MnCl_2·4H_2O$、 H_2SO_4、 HCl、NaOH、Glycine were all of analytical grade and used without further purification. Double deionized water was used throughout all the experiments.

Preparation of DNA-dots

Double-strand DNA (dsDNA) was water-dissolved in a sealed conical flask at

temperature of 85°C for 11h with the mild stirring and finally became single-strand DNA (ssDNA) under inert atmosphere. A 2mL quantity of the ssDNA/water solution was then injected into 2mL acetone while being sonicated in a water bath for a duration of 60min[12]. The suspension was filtered with a 0.2 μm membrane filter. The acetone was removed by partial evaporation under vacuum, followed by filtration through a 0.2 μm filter.

Cell culture

HeLa cells were employed in this article. Cells were cultured at 37°C in a CO_2 incubator by using Deulbecco's Modified Eagle Medium (DMEM) supplemented with 10% fetal bovine serum (FBS), 100μg/mL streptomycin and 100μg/mL penicillin.

MTT assay

An MTT assay was performed to test the toxicity of DNA-dots in a HeLa cell line. Cells were seeded into 96-well plates with a density of 1×10^5 cells/mL and incubated for 12h at 37°C. Then we treated the cells with various concentrations of DNA-dots and incubated for 24h. On the day of treatment, 20μL of MTT (1mg/mL stock solution in phosphate-buffered saline) was added into each well. After incubation at 37°C in a CO_2 incubator for 4h, MTT medium was removed and DMSO (150μL) was added to dissolve blue formazan crystals. We shake the plates for 15min to ensure mixing completely. Finally, the optical density (OD) values of the wells were determined at a test wavelength of 408nm.

Cell bioimaging of DNA-dots

HeLa cells were seeded into 24-well dishes and incubated at 37°C for 12h. On the day of treatment, different concentrations of DNA-dots were used for cells culture. After incubation for 24h, the residual medium on the coverslips were washed three times with 1× PBS, then inverted onto Superfrost Plus glass slides and sealed. Finally, fluorescence pictures of the cells were taken using a Leica TCS SP5 355nm ultraviolet light (UV) confocal microscope.

Characterization methods

The size and shape of the DNA-dots were characterized by Transmission electron microscopy (TEM), which the DNA-dots dispersion was dropped on ultra-thin copper grids. Elemental analysis was performed by X-ray photoelectron spectroscopy (XPS). A few drops of the DNA-dots solution was placed on the silicon substrate that had been sonicated for 1h in water and ethyl alcohol separately. After evaporation of the water, the surface was scanned with the instrument**s.**

TEM images were performed on a JEM-2100F transmission electron microscope with 200kV accelerating voltage. For further proving the product composition, X-ray photoelectron spectroscopy (XPS) was conducted on a Kratos Axis ULTRA X-ray photoelectron spectrometer with Al Ka X-ray as the excitation source. FTIR spectrum was carried out on a Thermo NEXUS 670 Fourier transform infrared spectrometer in the range of 400~4000cm^{-1}. The pH values were measured with a model pHS-3C pH meter. The fluorescence spectra were recorded with a RF-5301PC luminescence spectrometer using a 1cm quartz cell, and the UV-vis absorption spectra were collected with a Perkin Elmer Lamda 950 UV-vis spectrophotometer using

quartz cuvettes with an optical path of 1cm.

The quantum yield (by calibrating against quinine sulfate, excited at 288 nm) of the DNA-dots was 7.5%.

Results and discussion

Synthesis and characterization of DNA-dots

Preparation of the DNA-dots was schematically displayed in Fig.1a. DNA-dots were prepared using the protocol developed by Guo et al.[13] To further investigate the effect of the temperature on synthesis, a series of reactions was carried out where the ssDNA/water solution was heated at various temperatures (60~95°C). The fluorescence spectra of the DNA-dots obtained using different temperatures are shown in Fig. 1b. It is obvious that when the reaction temperature is 85°C, the fluorescence intensity is the strongest. In order to optimize the stirring time, different time (7~12h) was examined. As shown in Fig.1c, the optimal stirring time is 11h. The resultant DNA-dots were with excellent biocompatibility as well as water solubility and stored in the refrigerator for further characterization. The DNA-dots dispersion shows a blue fluorescence under UV lamp while the DNA dispersion reveals no fluorescence. Fig. 1d presents the excitation and emission spectra of DNA-dots, which DNA-dots were excited at 288nm and the maximum emission intensity observed at 408nm. Fig. 1e shows absorption peak at 264nm.

The fluorescence quantum yield (QY) was calculated by comparing the emission intensity between DNA-dots and quinine sulfate that in 0.1mol/L H_2SO_4 (QY=0.55), and the absorbance was kept below 0.05.

$$Yu = Ys \bullet \frac{Fu}{Fs} \bullet \frac{As}{Au}$$

Where Fu and Au are the integrated emission peak area and optical absorption of the DNA-dots, respectively. Fs and As are the integrated peak area and optical absorption of the quinine sulfate, and Yu and Ys are the fluorescence quantum yield for the DNA-dots and quinine sulfate, respectively.

Fig. 2a shows the transmission electron microscopy (TEM) image of the DNA-dots solution, which exhibits a substantially spherical shape and good dispersion. The HRTEM image (the upper right corner of the Fig. 2a) shows lattice fringes with an interplanar spacing of 0.22nm. Fig. 2b on the right side displays size distribution of the DNA-dots, we can see that diameters are about in the range of 2~6nm.

The functional groups of the as-abtained DNA-dots were characterized by FTIR spectroscopy. Fig. 3a exhibits the characteristic absorption band of stretching vibration of N–H at 3357cm^{-1} [6, 14-16], and the peak at 2853cm^{-1} is assigned to the C–H stretching vibration. The characterized peaks of the 1420cm^{-1} and 1253cm^{-1} C–N stretching vibration were observed. The peaks at 1103cm^{-1} and 1041cm^{-1} are both assigned to the C–O stretching vibrations, moreover, C=O stretching vibrations at 1650cm^{-1} and 1723cm^{-1}. XPS was further performed to analyze the surface state as well as elemental analysis of the DNA-dots. The wide scan XPS spectra in Fig. 3b show five peaks at 133.13, 187.86, 284.13, 400.13 and 532.13eV, which are attributed to P2p, P2s, C1s, N1s and O1s, respectively. The partial XPS spectra of O1s can be

resolved into four components centered at 530.9, 531.9, 532.5 and 533eV, which are attributed to the PO_4^{1-}[17,18], O=C, O–N[19] and O–C[20] bands (Fig. 3c), respectively. This suggests that the PO_4^{1-} groups on the backbone of DNA are well retained in the DNA-dots. The detailed C1s spectra (Fig. 3d) show four peaks corresponding to C–C, C–N, C–O and C=O. Two experimental results above coincide with each other[21].

Effect of solvent

Fig. 4 shows the absorption and emission spectra of DNA-dots in different solvents. The absorbance (258nm) and emission (325nm) bands of DNA-dots were founded in ether (EE) and dichloromethane (DCM) solutions. DNA-dots have undergone a red shift within 5nm in absorption spectra and about 30nm in emission spectra in the acetone (ACE, highly polar solvent). It was concluded that the most predominant factor which determines the difference of solvent shifts of fluorescence and absorption spectra of these molecules is the interaction energy between solute and solvent molecules due to orientation polarization[22].

Effect of pH

As shown in Fig. 5, the PL. intensities of as-prepared DNA-dots almost keep constant while increasing the pH value from 4.0 to 10.0, indicating DNA-dots are pH independent within this range. In addition, the emission spectrum of DNA-dots exhibits a blue shift in the emission peak with pH decreasing to 3.0, although the intrinsic emission bandwidth is unchanged. The shift of the emission peak may result from the conjugation between DNA-dots and H^+, and the decreased surface electric charge may decrease the orientation polarization rate and the Stokes shift[23]. So the pH

of the DNA-dots dispersion was kept from 6.0 to 8.0 by glycine - sodium chloride buffer solution in this paper.

Effect of ionic strength

We add the DNA-dots to different concentrations of the NaCl solution in order to investigate the fluorescence stability of DNA-dots under high ionic strength condition. Fig. 6 shows the fluorescence intensity was hardly changed when containing NaCl concentrations from 0 up to 400mmol/L. The results indicate the excellent stability of DNA-dots making it possible for sensing applications under physiological conditions.

Effect of other metal ionic

In order to evaluate the selectivity of the as-prepared DNA-dots, the performance of sensing system for metal ions was further investigated. Consequently, the fluorescence intensity changes in the presence of the representative metal ions were examined under the identical conditions, including Ag^{+}, Na^{+}, Cd^{2+}, Co^{2+}, Zn^{2+}, Ni^{2+}, Ca^{2+}, Fe^{2+}, Mn^{2+}, Cu^{2+}, Hg^{2+} Mg^{2+}, Cr^{3+}, Al^{3+} and Fe^{3+}, as shown in Fig. 7. The concentrations of all metal ions are 3000μmol/L. Fluorescence intensity is quenched completely when we add Fe^{3+} to the solution of DNA-dots. All those ions except Fe^{2+} and Mg^{2+} had no interference on the fluorescence of the DNA-dots. Although Fe^{2+} and Mg^{2+} ions could also quench the fluorescence to a certain degree, the interference on the quenching was negligible when they were coexisted with Fe^{3+} at low concentrations. The results indicate that the DNA-dots can be used for the selective detection of Fe^{3+}. This high selectivity of these DNA-dots for Fe^{3+} can be

obtained, probably because Fe^{3+} ions form complexes with PO_4^{3-} on the DNA-dots surface, and facilitate aggregation of the DNA-dots, causing fluorescence quenching.

Cell imaging applications of DNA-dots

For verifying the potential practicality of the as-obtained DNA-dots in biomedical applications, we selected HeLa cells as experimental subject. An MTT assay was used to evaluate the cytotoxicity of the DNA-dots. Fig. 8 shows the histograms of cell activity with various concentrations of DNA-dots. We can see that cell viability was not significantly decreased when cells were incubated with 50μg/mL DNA-dots for 24h, indicating DNA-dots possess well biological compatibility and low cytotoxicity. Based on the biocompatibility results, cell imaging applications of DNA-dots were further explored. The cell uptake behavior of DNA-dots was evaluated by Confocal Laser Scanning Microscopic (CLSM) observation[24]. The confocal microscope images of HeLa cells incubated with 10μg/mL of DNA-dots are shown in Fig. 9. Fig. 9a shows the bright field image, which indicated the HeLa cells still maintained normal morphology, showing the excellent biocompatibility of DNA-dots. We can clearly see the bright green fluorescence in the cytoplasm region (Fig. 9b) when excited with a 355nm laser. These results suggested facile uptake of DNA-dots by cells which are mainly located at the cytoplasm distinguished from nuclei. Consequently, the experiment demonstrates that DNA-dots could be used as cell imaging reagent and have promising potential for various biomedical applications. The experimental results show that DNA-dots could play a great role of the cytoplasmic marker and be applied to various biomedical researches.

Conclusion

In summary, a simple method was developed for the synthesis of remarkably water-soluble and monodispersed fluorescent DNA-dots. The as-prepared DNA-dots exhibited a strong fluorescence emission peak at 408nm and a quantum yield up to 7.5%. It is proposed that the fluorescence quenching mechanism is due to the complexes formed between DNA-dots and Fe^{3+}. We believe that the DNA-dots will be applied for promising applications in detection of Fe^{3+} and biological labeling.

Acknowledgement

This work was financially supported by the National Natural Science Foundation of China (Grant No. 21175117).

Notes and references

Figure Caption

Fig. 1

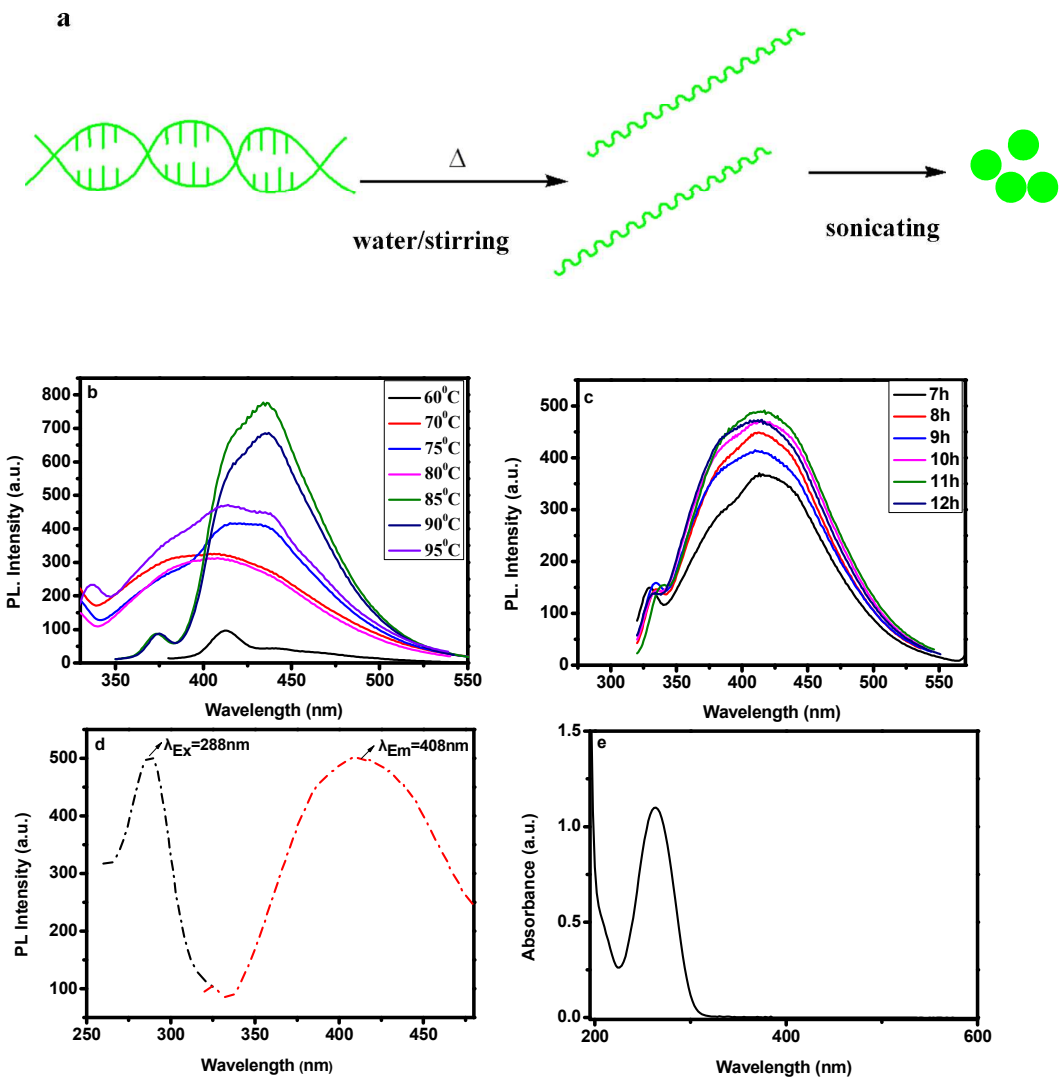

Fig. 1 (a) A schematic illustration of the preparation procedure of the DNA-dots (b) The fluorescence emission spectra of the DNA-dots at different reaction temperatures (c) The fluorescence emission spectra of the DNA-dots at different reaction time (d) Relevant fluorescence excitation and emission spectra and (e) The UV-Vis absorption spectrum.

Fig. 2

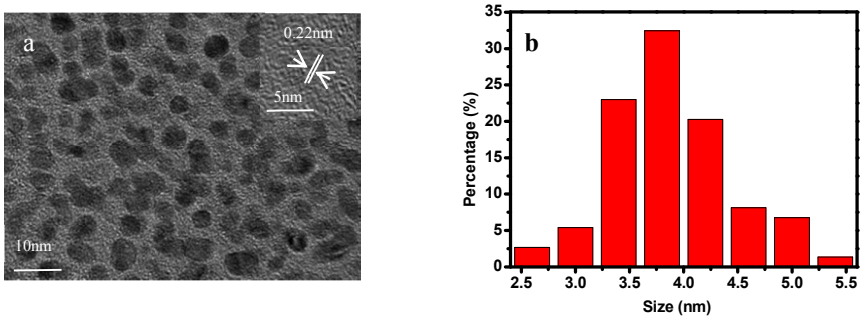

Fig. 2 (a) TEM image of DNA-dots. Inset of Fig. 2 (a): The HRTEM of DNA-dots. (b) The corresponding histograms of the nanoparticle size distribution.

Fig. 3

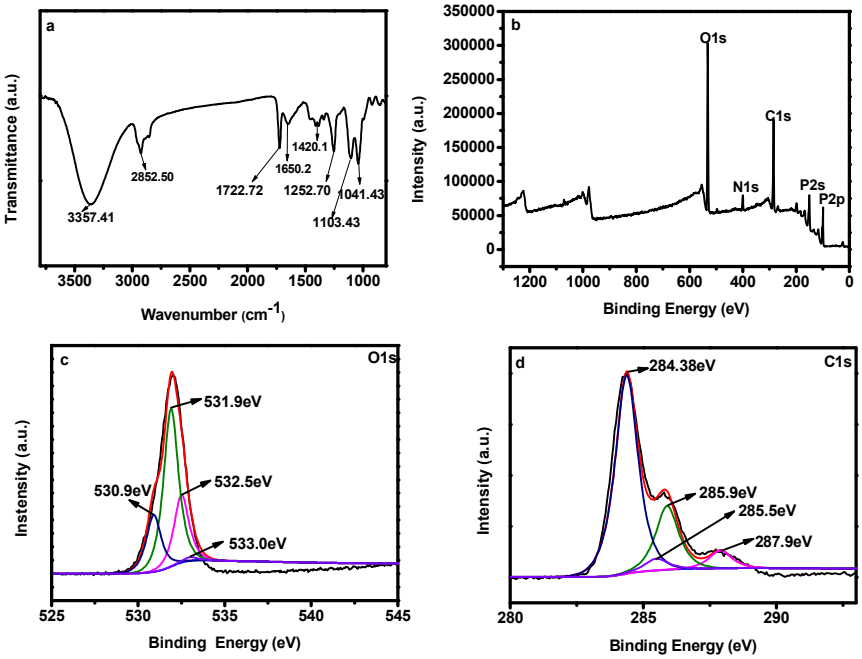

Fig. 3 (a) FTIR spectra of DNA-dots, (b) Survey XPS spectra of DNA-dots, (c) O1s and (d) C1s spectra of the DNA-dots.

Fig. 4

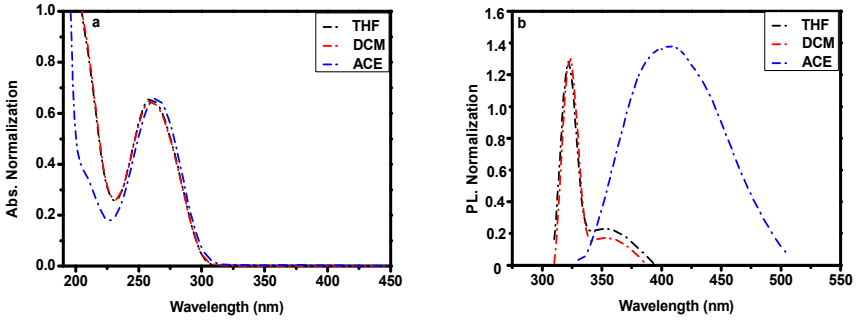

Fig. 4 UV–vis (a) and PL (b) Spectra of DNA-dots in different solvents (EE: ether; DCM: dichloromethane; ACE: acetone.)

Fig. 5

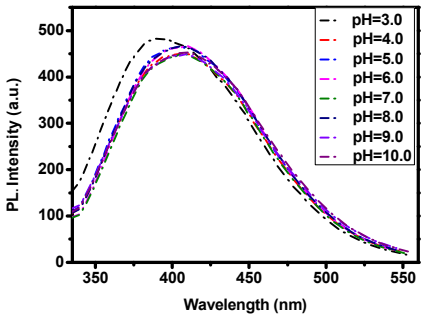

Fig. 5 The emission spectra of the DNA-dots at different pH values from 3.0 to 10.0.

Fig. 6

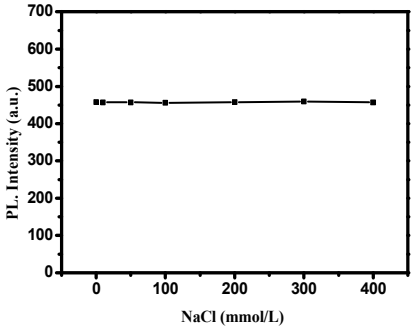

Fig. 6 The concentrations of NaCl (from 0 up to 400mmol/L) on DNA-dots fluorescence.

Fig. 7

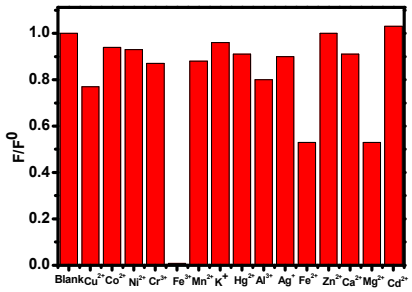

Fig. 7 The difference in fluorescence intensity at 408nm of DNA-dots dispersions between a blank solution and solutions containing different metal ions (excitation at 288nm; $[M^{n+}]$=3000μmol/L).

Fig. 8

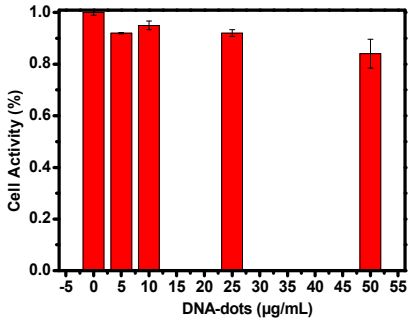

Fig. 8 Cell activity of different concentrations of DNA-dots with HeLa cells for 24h (n=5). Cell viability was determined by the MTT assay.

Fig. 9

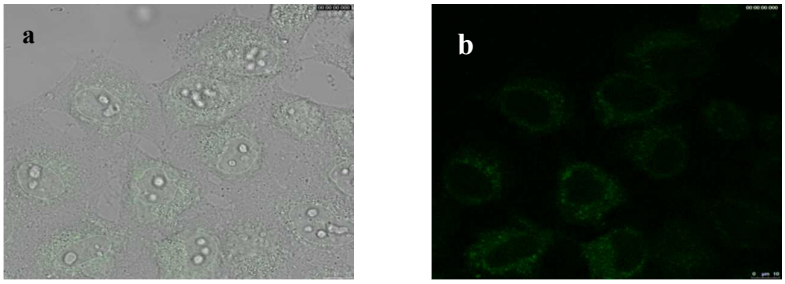

Fig. 9 Confocal microscope images of HeLa cells incubated with DNA-dots (10μg/mL) for 24h at 37°C. (a) Bright field; (b) Fluorescence image of cells excited with a 355nm laser.

1. Y.-H. Chan, Y. Jin, C. Wu and D. T. Chiu, *Chemical Communications*, 2011, **47**, 2820-2822.
2. Y. He, Z.-H. Kang, Q.-S. Li, C. H. A. Tsang, C.-H. Fan and S.-T. Lee, *Angewandte Chemie*, 2009, **121**, 134-138.
3. H. Shi, X. Ma, Q. Zhao, B. Liu, Q. Qu, Z. An, Y. Zhao and W. Huang, *Advanced Functional Materials*, 2014, **24**, 4823-4830.
4. C. Wu, S. J. Hansen, Q. Hou, J. Yu, M. Zeigler, Y. Jin, D. R. Burnham, J. D. McNeill, J. M. Olson and D. T. Chiu, *Angewandte Chemie International Edition*, 2011, **50**, 3430-3434.
5. H. Li, X. He, Y. Liu, H. Huang, S. Lian, S.-T. Lee and Z. Kang, *Carbon*, 2011, **49**, 605-609.
6. J. R. Dwyer, J. Dreyer, E. T. J. Nibbering and T. Elsaesser, *Chemical Physics Letters*, 2006, **432**, 146-151.
7. D. A. Limaye and Z. A. Shaikh, *Toxicology and Applied Pharmacology*, 1999, **154**, 59-66.
8. C. Yuan, M. Kadiiska, W. E. Achanzar, R. P. Mason and M. P. Waalkes, *Toxicology and Applied Pharmacology*, 2000, **164**, 321-329.
9. L. Deng, Z. Zhou, J. Li, T. Li and S. Dong, *Chemical Communications*, 2011, **47**, 11065-11067.
10. Z. Huang, F. Pu, Y. Lin, J. Ren and X. Qu, *Chemical Communications*, 2011, **47**, 3487-3489.
11. J. Sharma, H.-C. Yeh, H. Yoo, J. H. Werner and J. S. Martinez, *Chemical Communications*, 2010, **46**, 3280-3282.
12. C. Wu, C. Szymanski and J. McNeill, *Langmuir*, 2006, **22**, 2956-2960.
13. C. X. Guo, J. Xie, B. Wang, X. Zheng, H. B. Yang and C. M. Li, *Sci. Rep.*, 2013, **3**.
14. Ł. Szyc, J. R. Dwyer, E. T. J. Nibbering and T. Elsaesser, *Chemical Physics*, 2009, **357**, 36-44.
15. V. Kozich, Ł. Szyc, E. T. J. Nibbering, W. Werncke and T. Elsaesser, *Chemical Physics Letters*, 2009, **473**, 171-175.
16. T. Elsaesser, N. Huse, J. Dreyer, J. R. Dwyer, K. Heyne and E. T. J. Nibbering, *Chemical Physics*, 2007, **341**, 175-188.
17. T.-Z. Ren, Z.-Y. Yuan, A. Azioune, J.-J. Pireaux and B.-L. Su, *Langmuir*, 2006, **22**, 3886-3894.
18. L.-N. Feng, J. Peng, Y.-D. Zhu, L.-P. Jiang and J.-J. Zhu, *Chemical Communications*, 2012, **48**, 4474-4476.
19. O. Olivares, N. V. Likhanova, B. Gómez, J. Navarrete, M. E. Llanos-Serrano, E. Arce and J. M.
20. W. Li, Z. Zhang, B. Kong, S. Feng, J. Wang, L. Wang, J. Yang, F. Zhang, P. Wu, D. Zhao, Simple and Green Synthesis of Nitrogen-Doped Photoluminescent Carbonaceous Nanospheres for Bioimaging, Angewandte Chemie 125 (2013) 8309.
21. S. Stankovich, R. D. Piner, X. Chen, N. Wu, S. T. Nguyen and R. S. Ruoff, *Journal of Materials Chemistry*, 2006, **16**, 155-158.
22. N. Mataga, Y. Kaifu, M. Koizumi, Solvent Effects upon Fluorescence Spectra and the Dipolemoments of Excited Molecules, Bulletin of the Chemical Society of Japan,1956, 29 ,465.
23. D. Yu, Z. Wang, Y. Liu, L. Jin, Y. Cheng, J. Zhou, S. Cao, Quantum dot-based pH probe for quick study of enzyme reaction kinetics, Enzyme and Microbial Technology, 2007,41,127-132.
24. J. Xu, Y. Zhou, G. Cheng, M. Dong, S. Liu and C. Huang, *Luminescence*, 2014, n/a-n/a.